Addition of 8 analytical solutions to the SWASHES software

Maxime Rougier

INSTITUT ORLÉANS • TOURS Mathématiques & Physique Théorique DENIS POISSON

Addition of 8 analytical solutions to the SWASHES software

Maxime ROUGIER

August 16, 2022

Abstract

The Shallow-Water equations are a nonlinear system of partial differential equations commonly used to model flows in various contexts. Many solvers are being developed to numerically solve those equations, which raises the issue of the verification of the numerical results. To simplify the validation process, the software SWASHES was developed, compiling a significant number of analytical solutions to the Shallow-Water equations in a unified formalism to create an easily available and consistent set of test cases. The corresponding source codes are made available to the community (www.idpoisson.fr/swashes). In this report, we will describe the 8 new solutions implemented in version 1.04.00 of SWASHES. Adding both steady and transient solutions, with solutions in Cartesian geometry as well as solutions in spherical geometry.

Contents

Introduction

Shallow-Water equations have been proposed by Adhémar Barré de Saint-Venant in 1871 to model flows in a channel. Nowadays, they are widely used to model flows in various contexts, such as: overland flow, rivers, dam breaks, etc. These equations consist in a nonlinear system of partial differential equations (PDE-s), more precisely conservation laws describing the evolution of the height and mean velocity of the fluid. In real situations (realistic geometry, sharp spatial or temporal variations of the parameters in the model, etc.), there is no hope to solve explicitly this system of PDE-s. It is therefore necessary to develop specific numerical methods to compute approximate solutions of such PDE-s. Implementation of such methods raises the question of the verification of the code. Such validations are currently restricted because analytic solutions to the Shallow-Water equations are rare and have been published on an individual basis over a period of more than five decades. To solve this issue, the software SWASHES (Delestre et al. 2013) was developed, compiling a significant number of analytical solutions to the Shallow-Water equations in a unified formalism to create an easily available and consistent set of test cases. The corresponding source codes are made available to the community (www.idpoisson.fr/swashes). In this paper, we will describe the 8 new solutions implemented in the version 1.04.00 of SWASHES, a summary of those solutions is shown on table 1.

This paper should be considered an extension of Delestre et al. (2013). Thus, we will not go into details as to the implementation and usage of SWASHES. If you wish to use SWASHES, you should first read the aforementioned article. We will however briefly recall the global setting.

The Shallow-Water equations, also known as the Saint-Venant equations, are a set of partial differential equations. We recall the notations we use on figure 1. And give here the general setting of those equations as it is used in SWASHES, but many terms will be neglected in this paper:

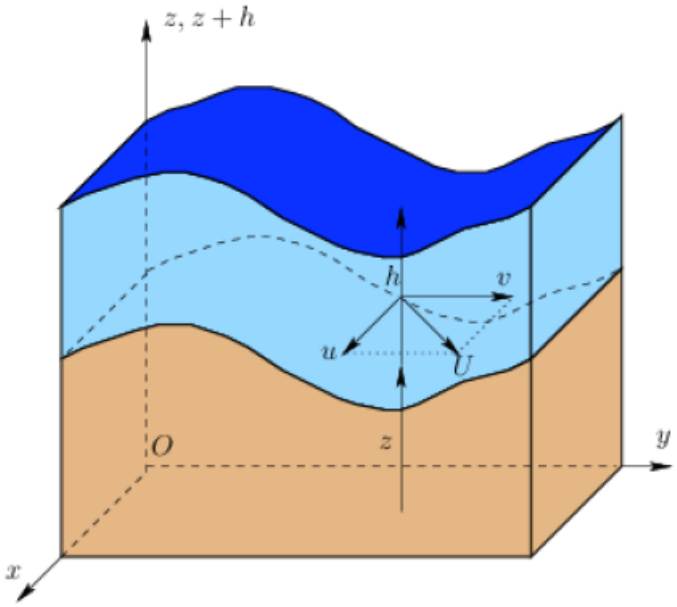

Figure 1: Notations for the Shallow-Water equations in 2D. Source: Delestre et al. (2013).

$$\begin{cases} \partial_t h + \partial_x(hu) + \partial_y(hv) = R - I \\ \partial_t(hu) + \partial_x\left(hu^2 + \frac{gh^2}{2}\right) + \partial_y(huv) = gh(-\partial_x z(x,y) - S_{fx}) + \mu S_{dx} \\ \partial_t(hv) + \partial_x(huv) + \partial_y\left(hu^2 + \frac{gh^2}{2}\right) = gh(-\partial_y z(x,y) - S_{fy}) + \mu S_{dy}, \end{cases} \tag{1}$$

where:

- g [L/T^2] is the gravitational acceleration. We set it as $g = 9.81$ m s^{-2}.
- $h(x, y, t)$ is the function of the water height [L].
- z is the topography [L]. Since we consider no erosion, it is a fixed function of space.
- (u, v) is the speed vector, where u is its component along x and v its component along$y$.
- $R \geq 0$ is the rain intensity [L/T], in this paper we always take $R = 0$.
- I is the infiltration rate [L/T], in this paper we always take $I = 0$.
- $S_f = (S_{fx}, S_{fy})$ is the friction force, in this paper we always take $S_F = 0$.
- $\mu S_d = (\mu S_{dx}, \mu S_{dy})$ is the viscous term where $\mu \geq 0$ is the viscosity of the fluid. We neglect for all the solutions in this paper.

New solutions				Time dependance		Coordinate system		Topography	
Type	Description	§	Reference	S.s.	Transitory	Cart.	Sph.	Flat	Variable
Dam at rest	Parabolic dam	1.1.1	See section 1	X		X			X
	Cross-shaped dam with a center well	4	See section 1	X		X			X
Global spherical model	Global S.s. Geostrophic Flow	1.2.1	Williamson et al. (1992)	X			X	X	
	Global S.s. Geostrophic Flow with an axial tilt	1.2.2	Williamson et al. (1992)	X			X	X	
Sluice gate opening problem with free flow	Opening on dry floor	2.2.1	Cozzolino et al. (2015)		X	X		X	
	Opening on slightly wet floor	2.2.2	Cozzolino et al. (2015)		X	X		X	
	Opening on wet floor	2.2.3	Cozzolino et al. (2015)		X	X		X	
Dam break problem with a step	Dam break with initial unmoving water	2.3	Han and Warnecke (2014)		X	X			X

Friction is always neglected; Cart.=Cartesian Sph.=Spherical S.s.=Steady state

Table 1: Summary of the new solutions implemented in version 1.04.00 of SWASHES.

1 Steady state solutions

In this section, we focus on 4 new steady state solutions in SWASHES, complementary to the ones already implemented (see Delestre et al. 2013, section 3). Steady state solutions being solutions that satisfy:

$$\partial_t(h) = \partial_t(hu) = \partial_t(hv) = 0.$$

1.1 Dam in 2D at rest

We implemented two new solutions consisting of two dam-like topographies in 2 dimensions at rest. As for all the new solutions, we here neglect friction and the viscosity term. We can then recall the shallow water equations in this case, by simplification of (1):

$$\begin{cases} \partial_x(hu) + \partial_y(hv) = 0 \\ \partial_x\left(hu^2 + \dfrac{gh^2}{2}\right) + \partial_y(huv) = -gh(\partial_x z(x,y)) \\ \partial_x(huv) + \partial_y\left(hu^2 + \dfrac{gh^2}{2}\right) = -gh(\partial_y z(x,y)). \end{cases}$$

We can see here that the solutions only depend on the topography $z(x, y)$ and the initial conditions. For the following solutions, we consider dam-like topographies, with initial water at rest retained by the dam in part of the domain and dry floor in the rest of the domain. The analytical solution in such a case is trivial, the water surface should stay flat and the velocity null. Such a test case has already been implemented in SWASHES (see Delestre et al. (2013), section 3.1), with the lake at rest. The aim of those solutions here is rather to take an initial condition with water in the whole domain and see if the numerical solution tends toward the analytical solution. One should especially focus on the transition between wet and dry domains, which is often a problem for numerical solvers. The main point of this section is to give a reference topography to allow such tests and make easy comparisons between different numerical solvers.

1.1.1 Parabolical dam

In this case, we look at a rectangular domain of length $L = 25$ m and width $l = 10$ m. The topography here is that of a classical parabolic dam ($x = (y - \frac{l}{2})^2/l^2 + dam_d$), see figure 2.

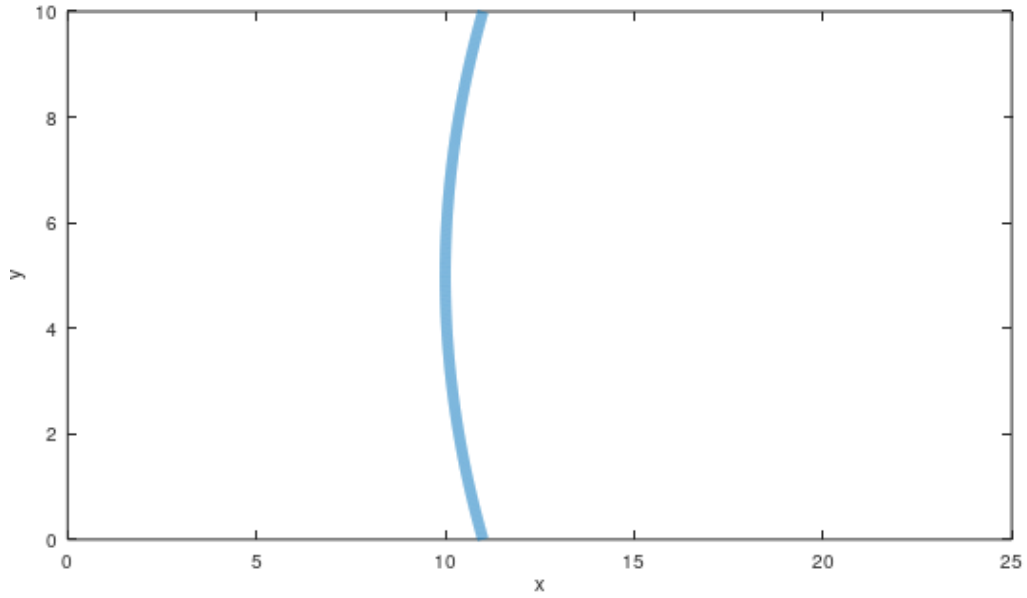

Figure 2: Shape of the dam from above.

For such a topography, we had to ensure that the ridge would be continuous, and always of the same height so that no water could pass through. To do so we added a flat surface on the top of the dam of width dam_w. If one chooses $dx \leq \frac{dam_w}{2}$, there will be at least two points of the mesh in the flat surface for any given y thus ensuring the continuity of the ridge. We will need another parameter we name dam_h, corresponding to the height of the dam.

To get such a topography, we chose a Gaussian curve with a truncated top and a slight offset at the base of the curve to set $z = 0$ m if $|x - dam_{center}| \geq 2dam_w$. The final shape is shown in figure 3 and given by the following formula:

$$z(x, y) = \min\left(0.5, \max\left(0, \frac{e^{-\phi(x,y)^2}}{\alpha} - \beta\right)\right). \tag{2}$$

Here α and β are parameters ensuring the chosen shape:

$$\begin{cases} \alpha = (e^{-(dam_w/2)^2} - e^{-2dam_w})/dam_h \\ \beta = e^{-(dam_w/2)^2}/\alpha - dam_h. \end{cases} \tag{3}$$

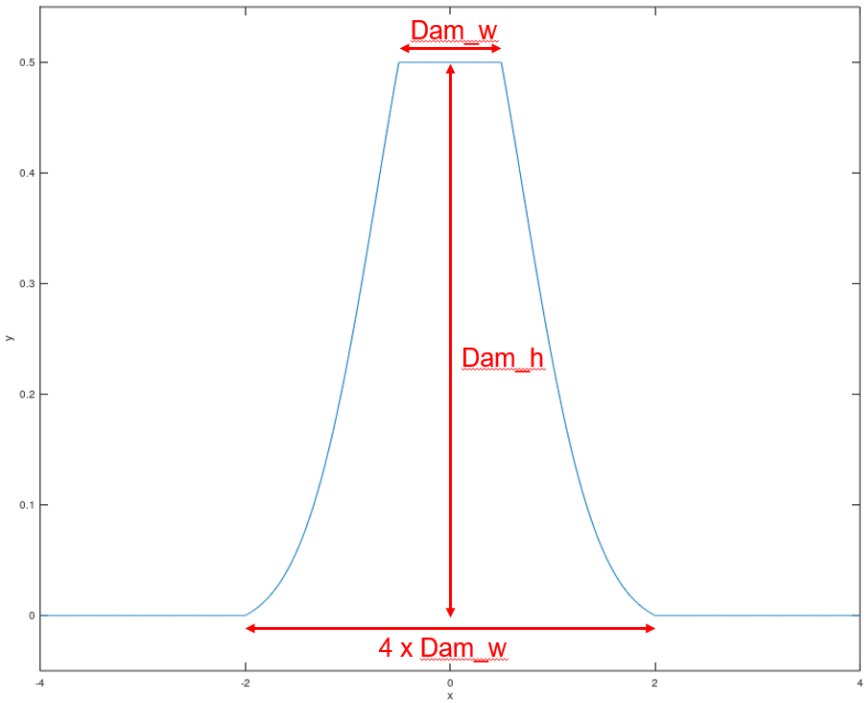

Figure 3: Cross-section of the dam.

To get the parabolic dam, we just have to fix $\phi(x, y)$:

$$\phi(x, y) = x - \frac{(y - l/2)^2}{l^2} - dam_d,$$

with dam_d corresponding to the distance between the upstream border and the center of the dam.

We then have to set the various parameters. For the Shallow-Water equations to be meaningful, we must have low water height compared to the horizontal dimensions of the domain. We chose $dam_h = 0.5$ m. Since we considered 50 minimum points for the subdivision of x was reasonable (*i.e.* $dx = 0.5$ m), we fix $dam_w = 1$ m. And since the wet-dry transition is the point of interest, we fixed the dry zone to be bigger: $dam_d = 10$ m.

As for the analytical solution itself, we have:

$$\begin{cases} h(x, y) + z(x, y) = 0.5 \text{ m if } g(x, y) \leq 0 \\ h(x, y) = 0 \text{ otherwise} \\ u(x, y) = 0 \\ v(x, y) = 0. \end{cases}$$

1.1.2 Cross-shaped dam

For this second dam, we keep the same cross-section as before (see figure 3) for the same reasons as in section 1.1.1. The shape from above is now a cross with a well in the center. As for the parameter that defines the shape of the dam (see equation (2)), dam_h still corresponds to the height of the dam, dam_w corresponds to its width and dam_d now corresponds to the radius of the center well.

Like the previous dam test case, the aim of this solution is to check whether the numerical solution tends toward the analytical solution, with the accent given on the symmetry of the solution. Since the topography is symmetrical horizontally, vertically, but also on the axes $x = y$ and $x = -y$, the numerical solution is expected to be symmetrical as well.

To compute the topography, we reuse formula (2), changing only the definition of the function $\phi(x, y)$. Implementation-wise, we treated the well and the cross part separately, obtaining respectively z_{ring} and z_{cross}. To simplify the following formula, we denote $\tilde{x} = x - \frac{L}{2}$ and $\tilde{y} = y - \frac{l}{2}$. We then get:

- For z_{ring}: $\phi(x, y) = \sqrt{\tilde{x}^2 + \tilde{y}^2} - dam_d$
- For z_{cross}: If $\sqrt{\tilde{x}^2 + \tilde{y}^2} > dam_d$, $\phi(x, y) = \min\left(\frac{|\tilde{x} - \tilde{y}|}{\sqrt{2}}, \frac{|\tilde{x} + \tilde{y}|}{\sqrt{2}}\right)$. Otherwise $z_{cross} = 0$.

We then compute the coefficients α and β (see (3)) with the following parameters:

- $dam_w = 1$ m, $dam_h = 1$ m and $dam_d = 2.5$ m for the well.
- $dam_w = 1$ m and $dam_h = 0.5$ m for the cross.

To get the total topography, we compute: $z(x, y) = \max(z_{ring}(x, y), z_{cross}(x, y))$. The topography is shown on figure 5.

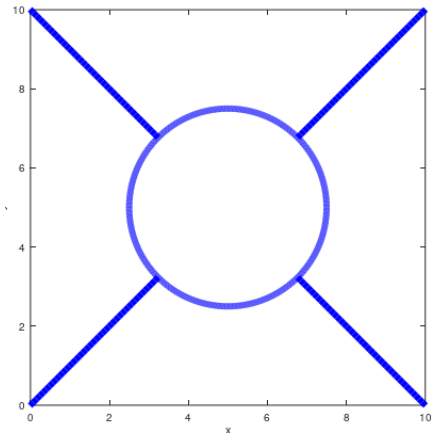

Figure 4: Shape of the dam from above.

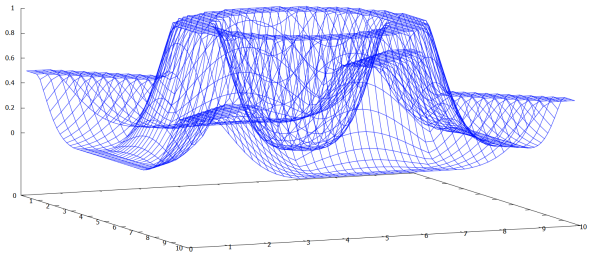

Figure 5: Topography of the cross-like dam.

1.2 Steady state solutions in spherical geometry

The Shallow-Water equations can be applied to any non-compressible fluids. In order to make global meteorological prediction, it is relevant to try to simulate oceans at a global scale. Such a model would require working at the scale of the whole planet, and thus to work in spherical coordinate systems. For this reason, people developed a form of Shallow-Water equations adapted to spherical geometry, and solver for these equations.

In order to broaden the scope of solutions implemented in SWASHES, we added two new solutions in spherical geometry.

This section is mainly based on Williamson et al. (1992), where the authors give several analytical solutions to the behavior of an incompressible and non-viscous fluid under different forces in spherical geometry, to serve as tests for numerical solvers.

We denote $\vec{i}$, $\vec{j}$ and $\vec{r}$ the longitudinal, latitudinal and radial vectors respectively. We will also denote λ and θ the longitudinal and latitudinal angles respectively, see figure 6.

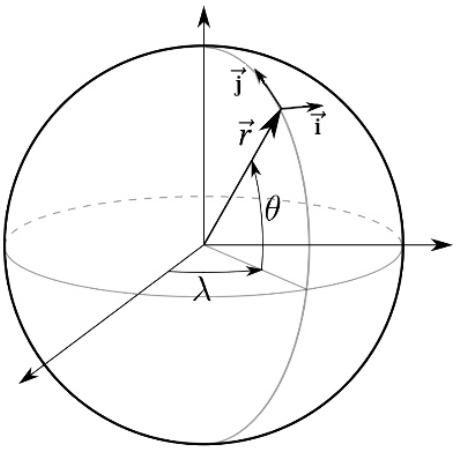

Figure 6: Spherical coordinate system.

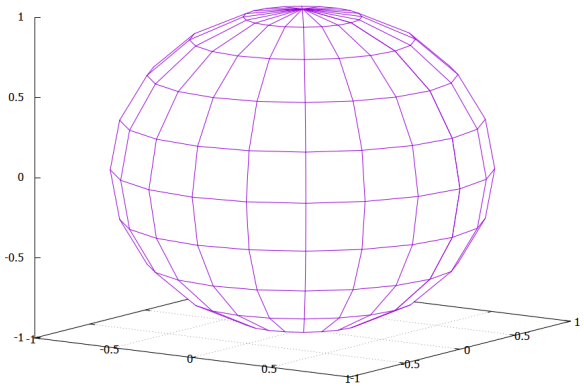

Figure 7: Spherical mesh.

From the general form of the Shallow-Water (1), it is possible to adapt them in spherical geometry. Those equations for a rotating sphere creating a Coriolis force are given by:

$$\begin{cases} \partial_t(h) + \nabla \cdot (h\mathbf{V}) = 0 \\ \partial_t(hu) + \nabla \cdot (hu\mathbf{V}) - \left(f + \dfrac{u}{a}\tan(\theta)\right) hv + \dfrac{gh}{a\cos(\theta)}\partial_\lambda(h+z) = 0 \\ \partial_t(hv) + \nabla \cdot (hv\mathbf{V}) - \left(f + \dfrac{u}{a}\tan(\theta)\right) hu + \dfrac{gh}{a}\partial_\theta(h+z) = 0. \end{cases} \tag{4}$$

Here $z(\lambda, \theta)$ [L] is the topography above a certain reference level (the sea-level), we consider it flat for the following solutions. We denote a [L] the radius of the reference level and $\mathbf{V}$ the speed vector $\binom{u}{v}$, where u and v [L/T] are its components along $\vec{i}$ and $\vec{j}$. Analogously, as for the Cartesian Shallow-Water equations, we consider that the velocity does not depend on its radial coordinates and the radial velocity component to be 0. The term f [L.M.T^{-2}] corresponds to the Coriolis force. Finally, as for the previous cases, $h(\lambda, \theta)$ [L] is the fluid height.

Since we are in spherical geometry, $\nabla\cdot$ is the spherical horizontal gradient operator given for any vector $(A, B)^T$ by:

$$\nabla \cdot \begin{pmatrix} A \\ B \end{pmatrix} \equiv \frac{1}{a\cos(\theta)}\Big(\partial_\lambda(A) + \partial_\theta(B\cos(\theta)\Big).$$

And for any scalar C, we have:

$$\mathbf{V} \cdot \nabla C \equiv \frac{u}{a\cos(\theta)}\partial_\lambda(C) + \frac{v}{a}\partial_\theta(C).$$

For the following test cases, we consider the sphere to be the Earth, that we will approximate to be a perfect sphere. We fix parameters close to the ones of Earth:

- $a = 6.37122 \times 10^6$ m Earth average radius (average between the equator and the poles).
- $\Omega = 7.292 \times 10^{-5}$ rad s^{-1} Earth's angular speed.
- $g = 9.81$ m s^{-2} the sea-level acceleration of gravity on Earth.

Since we now work in spherical geometry, we cannot use the Cartesian mesh already implemented in SWASHES. We chose to use the most widely used mesh for spherical geometry, see figure 7, described below. As for the other solutions, when using SWASHES, the user chooses N_x and N_y. But in the case of the spherical mesh, they will correspond to the number of subdivisions for λ and θ. Since we consider the simplest mesh, those subdivisions are uniform, so we get $d\lambda = 2\pi/N_x$ and $d\theta = \pi/(N_y - 1)$. SWASHES then computes h, u and v at each point of the mesh, those points being defined for the following angles: $\lambda = n \times d\lambda$ and $\theta = m \times d\theta$, where $0 \leq n \leq N_x$ and $0 \leq n \leq N_y - 1$ are integers.

To correctly represent the result, we require that λ goes from 0 to 2π. Since the points $\lambda = 2\pi$ do not add new information, we chose to not take them into account in the number of points selected. Thus, SWASHES will actually do $(N_x+1) \times N_y$ computations. But considering what was just said and the fact that all points of form $(\lambda, 0)$ and $(\lambda, 2\pi)$ correspond to the lower and upper pole respectively, the mesh will actually contain only $N_x \times (N_y - 2) + 2$ distinct points.

1.2.1 Global geostrophic steady state with no axial tilt

In the first case we do not take the axial tilt into account, we consider the rotation axis is equal to the poles' axis. We also consider that the planet is in a global geostrophic steady state. A geostrophic current or flow is a current in which the pressure gradient force is balanced by the Coriolis effect. Usually, the fluid naturally tends to move from a region of high pressure (or high sea level) to a region of low pressure (or low sea level). The force pushing the water towards the low pressure region is called the pressure gradient force. But in a geostrophic flow, instead of fluid moving from a region of high pressure (or high sea level) to a region of low pressure (or low sea level), it moves along the lines of equal pressure (isobars). This occurs because the Earth is rotating. The rotation of the Earth results in the Coriolis force being applied on the fluid. The Coriolis force acts at right angles to the flow, and when it balances the pressure gradient force, the resulting flow is known as geostrophic. In practice, the oceanic flow outside the tropics is almost always in quasi-geostrophic equilibrium.

In this case, the Coriolis force is given by:

$$f = 2\Omega \sin(\theta).$$

We set initial conditions close to the real average value for Earth:

- $h_0 = 3000$ m height of the fluid above sea level.
- $u_0 = 2\pi a/(12 \text{ days}) \approx 38.61 \text{ m s}^{-1}$ initial speed of the fluid.

Considering the solution is a steady state, we can find the following analytical solution to (4):

$$\begin{cases} u = u_0 \cos(\theta) \\ v = 0 \\ h = h_0 - \left(a\Omega u_0 + \dfrac{u_0^2}{2}\right) \times \dfrac{(\sin(\theta))^2}{g}. \end{cases}$$

Here we find speed parallel to the latitude lines, the velocity component along $\vec{j}$ is 0. The fluid height is higher around the equator, see figure 8.

1.2.2 Global geostrophic steady state with an axial tilt

This second case is nearly identical to the first one, the only difference being a slight angle offset between the rotation axis of the sphere and the coordinate system poles that we note η. We approximate $\eta = 0.406$ rad constant, this value is close to Earth's average axial tilt. We can apply a change of coordinate system to the solution we previously found to find the analytical solution to this new problem. The Coriolis force is now given by:

$$f = 2\Omega(-\cos(\lambda)\cos(\theta)\sin(\eta) + \sin(\theta)\cos(\eta)).$$

We keep the same initial conditions as the previous section 1.2.1 ($h_0 = 3000$ m and $u_0 = 38.61 \text{ m s}^{-1}$) and we obtain:

$$\begin{cases} u = u_0(\cos(\theta)\cos(\eta) + \cos(\lambda)\sin(\theta)\sin(\eta)) \\ v = -u_0 \sin(\lambda)\sin(\eta) \\ h = h_0 - \left(a\Omega u_0 + \dfrac{u_0^2}{2}\right) \times \dfrac{(-\cos(\lambda)\cos(\theta)\sin(\eta) + \sin(\theta)\cos(\eta))^2}{g}. \end{cases}$$

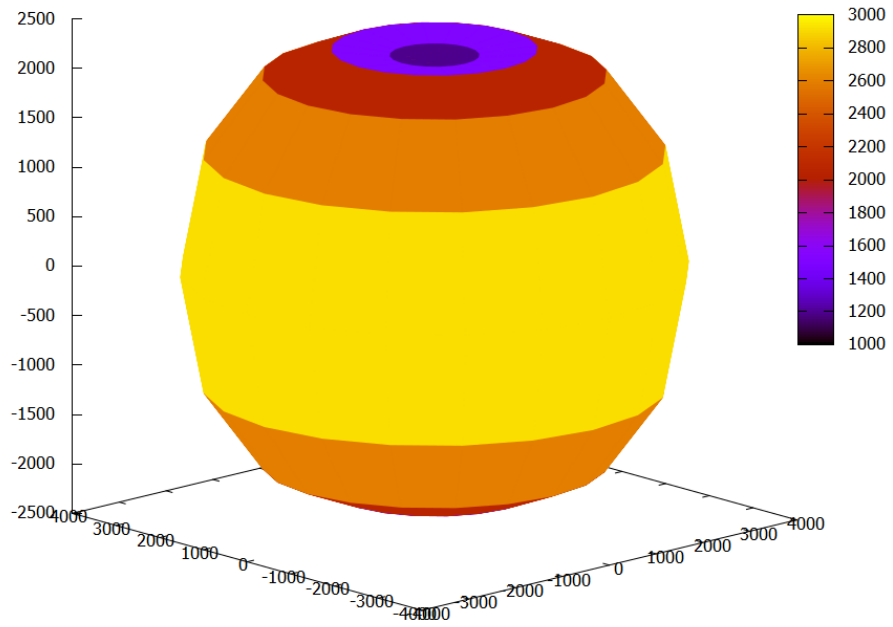

Figure 8: Height of the fluid at the geostrophic steady state.

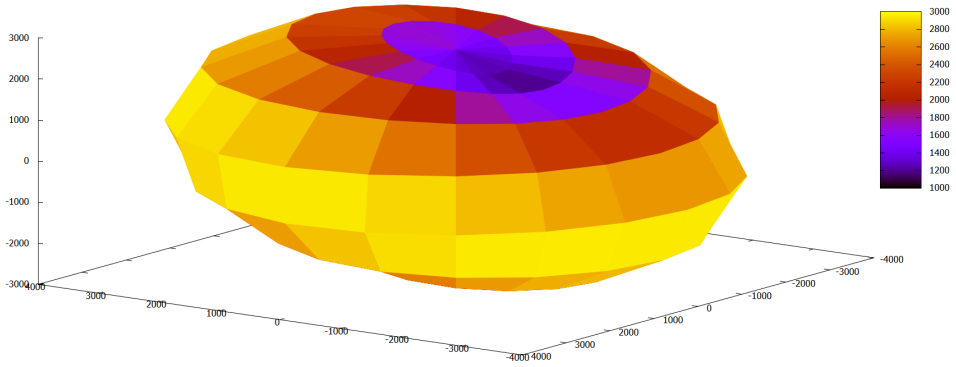

Figure 9: Height of the fluid at the geostrophic steady state with an axis tilt.

The solution is exactly the same as before, simply with an offset between the axis of rotation of the sphere and the coordinate system poles. This case is interesting because the mesh we chose (see figure 7) strongly focuses on the poles, while the solution does not, giving the results shown on figure 9.

2 Transitory solutions

In this section, we focus on 1 dimension transitory solutions. We implemented solutions to two variations of the dam break problem (also called Riemann problem). See Delestre et al. (2013) section 4.1 to see the solutions to the different Riemann problems already implemented in SWASHES (on dry or wet floor, with or without friction).

To solve such problems, we once again work with the Shallow-Water equations in the Cartesian coordinate system (1). We consider the solution to be transitory, without friction, with non-viscous water and the topography is flat (except for the solution with a step, where it is flat everywhere apart except at the step where there is a discontinuous jump). We recall the Shallow-Water equations in

such a case:

$$\begin{cases} \partial_t h + \partial_x(hu) = 0 \\ \partial_t(hu) + \partial_x\left(hu^2 + \frac{gh^2}{2}\right) = 0. \end{cases}$$

2.1 Elements of resolution: The classical Riemann problem

Before describing the new transitory solutions implemented in SWASHES it is relevant to start by studying the simpler case of the classical Riemann problem. In this section we will give elements of resolution useful for all the new solutions as well as the solution of a Riemann problem as an illustration of the method of resolution.

In the classical Riemann problem, for the dam break resolution, we initially consider a domain in one dimension, divided in its center by a dam, represented by a discontinuity between the left state and the right state. The goal is to find the behavior of the water in time once we remove the dam at $t = 0$ s.

As we said earlier, we take a domain divided in two at the center point (the abscissa of the dam), we denote it x_0. In the rest of this paper, the indices L and R refer to the left side and right side of the dam respectively. We also note $\mathbf{U}(x,t) = (h(x,t) \;\; u(x,t))^T$, the vector describing the state of the solution at a set position and time. Initially we have:

$$\mathbf{U}(x,0) = \begin{cases} \mathbf{U}_L, \; x < x_0 \\ \\ \mathbf{U}_R, \; x > x_0 \end{cases} \qquad \mathbf{U}_L = (h_L \; u_L)^T, \; \mathbf{U}_R = (h_R \; u_R)^T.$$

To be consistent with the rest of SWASHES solutions, we set $L = 10$ m, and we fix $h_L > h_R$, so that the water flows from the left to the right. We make this choice without loss of generality, if one wants the solution to a problem of form $h_L < h_R$, they can just apply a symmetry around $x = x_0$.

The solution is transitory, but comparing the numerical solution to the analytical solution at every time is quite heavy. We instead set a reference time T, at which we give the solution. The choice made in SWASHES is: $T = 6$ s.

2.1.1 The different kind of waves

One can show (Alcrudo and Benkhaldoun 2001), that two different stable states $\mathbf{U}_1$ and $\mathbf{U}_2$ in such a problem are always linked by one of two kind of wave: either a shock wave, which we note $S(\mathbf{U}_1, \mathbf{U}_2)$, or a rarefaction wave, which we note $R(\mathbf{U}_1, \mathbf{U}_2)$.

Each kind of wave possesses a locus of admissible state in the plane (h, u) :

$$S(\mathbf{U}_1, \mathbf{U}_2) \;\; u_2 = u_1 \pm (h_2 - h_1)\sqrt{\frac{g}{2}\left(\frac{1}{h_1} + \frac{1}{h_2}\right)}$$

$$R(\mathbf{U}_1, \mathbf{U}_2) \;\; u_2 = u_1 \pm 2\left(\sqrt{gh_1} - \sqrt{gh_2}\right).$$

In both cases, we use the $+$ sign if $h_2 < h_1$, and the $-$ sign if $h_2 > h_1$. Both curves are useful to find the intermediate state between $\mathbf{U}_L$ and $\mathbf{U}_R$.

For a rarefaction wave between the state $\mathbf{U}_1$ and the state $\mathbf{U}_2$, one can also find the expression of $h(x,t)$ and deduce the expression of $u(x,t)$ using $R(\mathbf{U}_1, \mathbf{U}_2)$. Here we have x_0 the starting point of the wave: in all the cases we look at, it corresponds to the position of the dam:

$$h(x,t) = \begin{cases} \frac{1}{9g}\left(u_1 + 2\sqrt{gh_1} - \frac{x-x_0}{t}\right)^2 \\ \\ \frac{1}{9g}\left(u_2 - 2\sqrt{gh_2} - \frac{x-x_0}{t}\right)^2 \end{cases} \quad u(x,t) = \begin{cases} \frac{2}{3}\left(\frac{u_1}{2} + \sqrt{gh_1} + \frac{x-x_0}{t}\right) & \text{if } h_1 > h_2 \\ \\ \frac{2}{3}\left(-\frac{u_2}{2} + \sqrt{gh_2} + \frac{x-x_0}{t}\right) & \text{if } h_1 < h_2. \end{cases} \tag{5}$$

To find $x_1(t)$ and $x_2(t)$ the points of beginning and end of the wave, we solve: $h(x_1(t), t) = h_1$ and $h(x_2(t), t) = h_2$, which gives for example in the first case: $x_1(t) = x_0 + t(u_1 - \sqrt{gh_1})$.

For a shock wave between the state $\mathbf{U}_1$ and the state $\mathbf{U}_2$, there is no expression for the height since the wave is forms a discontinuity from $\mathbf{U}_1$ to $\mathbf{U}_2$. So one just needs to know the speed σ of the wave, which is given by the following formula:

$$\sigma = u_1 \pm h_2 \sqrt{\frac{g}{2}\left(\frac{1}{h_1} + \frac{1}{h_2}\right)}. \tag{6}$$

Here too, we use the sign + if $h_2 < h_1$, and the − sign if $h_2 > h_1$. Once we know its speed, the position of the wave discontinuity is given by: $x_0 + t\sigma$.

As it is explained in LeVeque (2002), once those wave equations are known, the difficulty of solving Riemann problems lies in finding the number of intermediate states and finding what kind of waves links them together. Afterwards, we can find the intermediate states at the intersection between the locus of the waves connecting them to the other state. The solution is then entirely known, since we know $\mathbf{U} = (h\ u)^T$ for each stable state, and we can find it for the waves using (5) and (6).

2.1.2 Example of the Riemann problem for the complete dam break

With those equations known, we can now tackle the resolution of a Riemann problem. Since we want to simulate a dam break, we choose zero speed initial conditions, such that $u_L = u_R = 0$. In this case, we obtain three different states (see Alcrudo and Benkhaldoun (2001, section 5)): $\mathbf{U}_L$ and $\mathbf{U}_R$ that we know, as well as $\mathbf{U}_1$ an intermediate state. The left state is linked to the intermediate state via a rarefaction wave, and the right state is linked to the intermediate state via a shock. In the rest of this paper, we reuse the notations proposed by (Alcrudo and Benkhaldoun 2001), we write the different states with an arrow indicating what kind of wave links them to the next state:

$$\mathbf{U}_L \xrightarrow{R} \mathbf{U}_1 \xrightarrow{S} \mathbf{U}_R.$$

The state $\mathbf{U}_1$ is found at the intersection of $R(\mathbf{U}_L, \mathbf{U})$ and $S(\mathbf{U}, \mathbf{U}_R)$ in the (h, u) plane, where $\mathbf{U}$ is the state we want to find. We have $h_R < h < h_L$, so one must pay attention to use the correct signs in the wave functions. To find the intersection, several methods are possible: for the sake of simplicity we used a simple dichotomy in SWASHES. The solution is then given as follows:

$$h(x,t) = \begin{cases} h_L \\ \frac{1}{9g}\left(2\sqrt{gh_L} - \frac{x-x_0}{t}\right)^2 \\ h_1 \\ h_R \end{cases} \qquad u(x,t) = \begin{cases} 0 & \text{if } x \le x_1(t) \\ \frac{2}{3}\left(\sqrt{gh_L} + \frac{x-x_0}{t}\right) & \text{if } x_1(t) \le x \le x_2(t) \\ u_1 & \text{if } x_2(t) \le x \le x_3(t) \\ 0 & \text{if } x_3(t) < x. \end{cases}$$

- $x_1(t) = x_0 - t\sqrt{gh_L}$
- $x_2(t) = x_0 - t(3\sqrt{gh_1} - 2\sqrt{gh_L})$
- $x_3(t) = x_0 + t\left(u_1 + h_R\sqrt{\frac{g}{2}\left(\frac{1}{h_1} + \frac{1}{h_R}\right)}\right)$.

This solution corresponds to the one already implemented in SWASHES where we chose $\mathbf{U}_L = (0.05\ 0)^T$ and $\mathbf{U}_R = (0\ 0)^T$. The solution is drawn on figure 10 at $t = T = 6$ s.

2.2 Analytical solutions to a Riemann problem with a sluice gate

In this section, we consider the Riemann problem with a sluice gate. We solved the classical Riemann problem in section 2.1 and defined several useful equations and notations that we reuse in this section. This section is mostly based on Cozzolino et al. (2015).

We take a closer look at the sluice-gate problem. Here, instead of the whole dam breaking, we consider that only a part opens at the bottom of size b, allowing only some water to flow through. We note x_0 the position of the sluice gate. We initially consider a domain in one dimension, divided

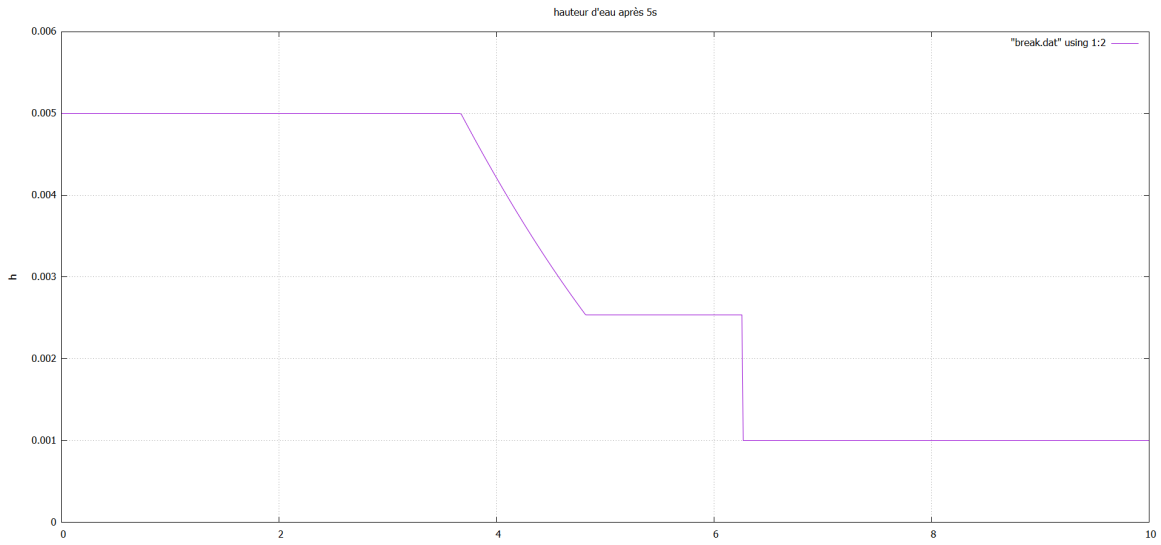

Figure 10: Curve of the water height after a dam break at $t = T = 6$ s.

in its center by a dam, represented by a discontinuity between the left state and the right state. The goal is to find the behavior of the water in time once we open the sluice gate at $t = 0$ s:

$$\mathbf{U}(x,0) = \begin{cases} \mathbf{U}_L, \ x < x_0 \\ \\ \mathbf{U}_R, \ x > x_0 \end{cases} \qquad \mathbf{U}_L = (h_L \ u_L)^T, \ \mathbf{U}_R = (h_R \ u_R)^T.$$

We keep the same convention as before with a domain of length $L = 10$ m and water flowing from left to right with $h_L > h_R$. To find a solution with $h_L < h_R$, one just needs to apply a symmetry at center with the analytical solution. Since we want to model the sudden opening of the sluice gate, we chose zero speed initial conditions, such that $u_L = u_R = 0$. We also consider that $b < h_L$ otherwise the solution just corresponds to the classical Riemann problem. Finally, we set the reference time in SWASHES as $T = 6$ s to compare with the numerical solution.

For a flow through an orifice, we observe a decrease in the flow surface after the orifice. The point where the flow surface is the lowest is called the Vena Contracta (see figures 11 and 12). To model this phenomenon, we introduce the contraction coefficient C_c, which is the ratio between the size of the jet and the size of the orifice. We note $\mathbf{U}_c = (h_c \ u_c)$ the state found right after the sluice gate, and we have $h_c = C_c b$.

In order to analytically solve the problem, some hypothesis were given in Cozzolino et al. (2015) that we keep:

- H1: the Froude similarity is valid. Meaning that the Froude number ($Fr = \frac{u}{gh}$) is similar between the theoretical model and in practice.
- H2: the energy is conserved across the sluice-gate.
- H3: the contraction coefficient does not depend on the relative opening of the gate, and it is constant during the transient. In the rest we set $C_c = 0.611$ as is suggested in Cozzolino et al. (2015).

The flow coming out of the sluice gate can be either free or submerged. We chose here to only look at free flow solutions, meaning that the flow coming out of the sluice is exposed to the air. In such case, we can show that the discharge q only depends on h_L and the size of the opening b. We get the following formula for q:

$$q = \frac{C_c}{\sqrt{1 + \frac{C_c b}{h}}} b\sqrt{2gh}. \tag{7}$$

Since $q = hu$, we can define a locus of admissible state at the sluice gate in the (h, u) plane. We

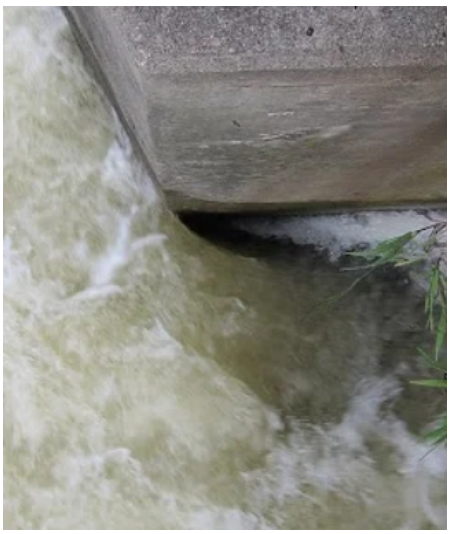

Figure 11: Illustration of the Vena Contracta phenomenon. Source: Mecholic (2018).

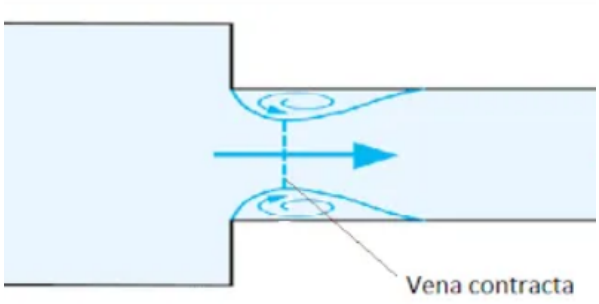

Figure 12: Scheme of the Vena Contracta. Source: Mecholic (2018).

denote it $FF(\mathbf{U})$:

$$FF(\mathbf{U}) \;\; u = \frac{C_c}{\sqrt{1+\frac{C_c b}{h}}}\frac{b}{h}\sqrt{2gh}.$$

We define another useful curve in the (h,u) plane, the curve of constant discharge $CD(q,\mathbf{U})$:

$$CD(q,\mathbf{U}) \;\; u = \frac{q}{h}.$$

Finally it is shown in Cozzolino et al. (2015) that if $b \geq \frac{4}{9}h_L$, there might be some non orifice flow, solutions in which the water does not interact with the sluice gate. In such cases, we find the same solutions as in 2.1.2. Since this case has already been implemented in SWASHES, we chose here to work only on orifice solution by fixing $b = 0.2h_L$.

2.2.1 Free flow solution on dry domain

The first case we look at is the opening of the sluice gate on a dry domain, $h_R = 0$ m. In this case we obtain four different states, with a solution of the form:

$$\mathbf{U}_L \xrightarrow{R} \mathbf{U}_1 \xrightarrow{CD} \mathbf{U}_c \xrightarrow{R} \mathbf{U}_R.$$

The state $\mathbf{U}_1$ lies at the intersection between $R(\mathbf{U}_L,\mathbf{U})$ and $FF(\mathbf{U})$ since $\mathbf{U}_1$ is the state directly upstream of the dam and must then satisfy equation (7). Once $\mathbf{U}_1$ has been found, we know that $\mathbf{U}_c$ lies in $CD(h_1u_1,\mathbf{U})$ since the discharge through the gate is constant. The state $\mathbf{U}_c$ is then individuated by $h_c = C_c b$. We obtain the following solution:

$$h(x,t) = \begin{cases} h_L \\ \frac{1}{9g}\left(2\sqrt{gh_L} - \frac{x-x_0}{t}\right)^2 \\ h_1 \\ h_c \\ \frac{1}{9g}\left(u_c + 2\sqrt{gh_c} - \frac{x-x_0}{t}\right)^2 \\ 0 \end{cases} \qquad u(x,t) = \begin{cases} 0 & \text{if } x \leq x_1(t) \\ \frac{2}{3}\left(\sqrt{gh_L} + \frac{x-x_0}{t}\right) & \text{if } x_1(t) \leq x \leq x_2(t) \\ u_1 & \text{if } x_2(t) \leq x \leq x_0 \\ u_c & \text{if } x_0 \leq x \leq x_3(t) \\ \frac{2}{3}\left(\frac{u_1}{2} + \sqrt{gh_1} + \frac{x-x_0}{t}\right) & \text{if } x_3(t) \leq x \leq x_4(t) \\ 0 & \text{if } x_4(t) < x, \end{cases}$$

where:

- $x_0 = 5$ m
- $x_1(t) = x_0 - t\sqrt{gh_L}$

- $x_2(t) = x_0 - t(3\sqrt{gh_1} - 2\sqrt{gh_L})$
- $x_3(t) = x_0 + t(u_c - \sqrt{gh_c})$
- $x_4(t) = x_0 + t(u_c + 2\sqrt{gh_c})$.

In SWASHES, we set $h_L = 0.005$ m, $h_R = 0$ m, $C_c = 0.611$ and $b = 0.2h_L$. This solution is represented at $t = T = 6$ s, in figure 13.

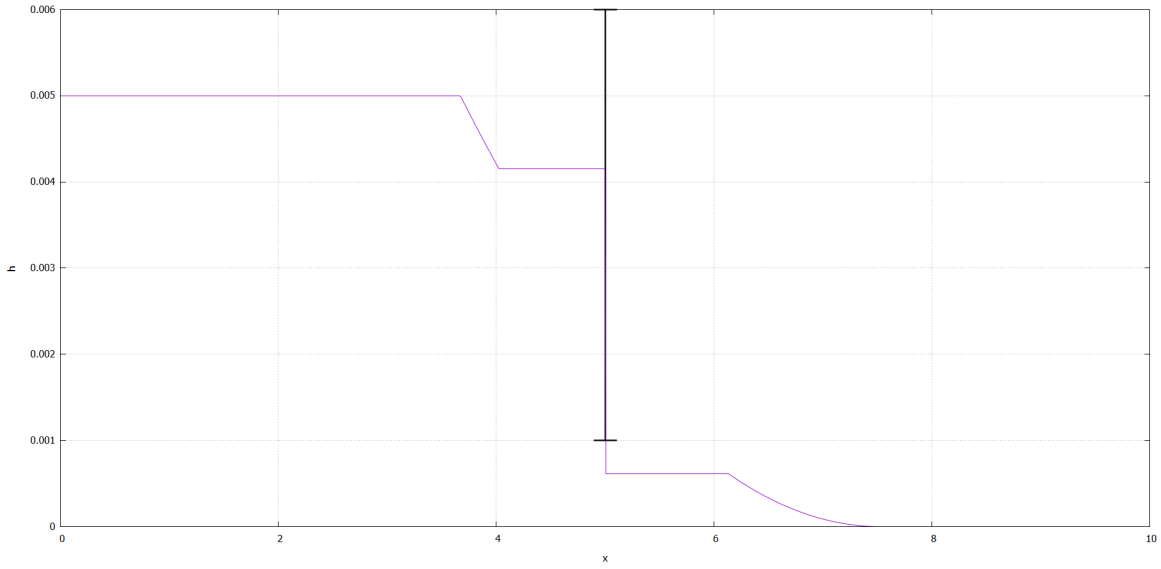

Figure 13: Free flow solution on dry domain at $t = T = 6$ s.

2.2.2 Free flow solution on slightly wet domain ($h_R < h_c$)

In this solution, we take a non-zero h_R. We obtain two different solutions depending on whether $h_R < h_c$ or $h_R > h_c$.[1]

Here we set ourselves in the slightly wet case where $h_R < h_c$. The solution upstream of the dam is the same as for the dry domain, we still have $\mathbf{U}_L$ and $\mathbf{U}_1$ linked by a rarefaction wave. We find $\mathbf{U}_1$ at the intersection between $R(\mathbf{U}_L, \mathbf{U})$ and $FF(\mathbf{U})$. Downstream, we obtain a new intermediate state $\mathbf{U}_2$ between $\mathbf{U}_c$ and $\mathbf{U}_R$, with $h_c > h_2 > h_R$. The solution is of the form:

$$\mathbf{U}_L \xrightarrow{R} \mathbf{U}_1 \xrightarrow{CD} \mathbf{U}_c \xrightarrow{R} \mathbf{U}_2 \xrightarrow{S} \mathbf{U}_R.$$

We find $\mathbf{U}_c$ on $CD(h_1u_1, \mathbf{U})$ individuated by $h_c = C_c b$. Finally, $\mathbf{U}_2$ is found at the intersection between the curves $R(\mathbf{U}_c, \mathbf{U})$ and $S(\mathbf{U}, \mathbf{U}_R)$. We obtain the following solution:

$$h(x,t) = \begin{cases} h_L \\ \frac{1}{9g}\left(2\sqrt{gh_L} - \frac{x-x_0}{t}\right)^2 \\ h_1 \\ h_c \\ \frac{1}{9g}\left(u_c + 2\sqrt{gh_c} - \frac{x-x_0}{t}\right)^2 \\ h_2 \\ h_R \end{cases} \qquad u(x,t) = \begin{cases} 0 & \text{if } x \le x_1(t) \\ \frac{2}{3}\left(\sqrt{gh_L} + \frac{x-x_0}{t}\right) & \text{if } x_1(t) \le x \le x_2(t) \\ u_1 & \text{if } x_2(t) \le x \le x_0 \\ u_c & \text{if } x_0 \le x \le x_3(t) \\ \frac{2}{3}\left(\frac{u_1}{2} + \sqrt{gh_1} + \frac{x-x_0}{t}\right) & \text{if } x_3(t) \le x \le x_4(t) \\ u_2 & \text{if } x_4(t) \le x \le x_5(t) \\ 0 & \text{if } x_5(t) < x, \end{cases}$$

where:

- $x_0 = 5$ m
- $x_1(t) = x_0 - t\sqrt{gh_L}$

[1] If $h_R = h_c$, solutions 2.2.2 and 2.2.3 are equivalent, giving $\mathbf{U}_c = \mathbf{U}_2$ linked to $\mathbf{U}_R$ by a shock.

- $x_2(t) = x_0 - t(3\sqrt{gh_1} - 2\sqrt{gh_L})$
- $x_3(t) = x_0 + t(u_c - \sqrt{gh_c})$
- $x_4(t) = x_0 + t(u_c - 3\sqrt{gh_2} + 2\sqrt{gh_c})$
- $x_5(t) = x_0 + t\left(u_2 + h_R\sqrt{\frac{g}{2}\left(\frac{1}{h_2} + \frac{1}{h_R}\right)}\right)$.

In SWASHES, we set $h_L = 0.005$ m, $b = 0.2h_L$, $h_R = 0.002h_L$ and $C_c = 0.611$. This solution is represented at $t = T = 6$ s, in figure 14.

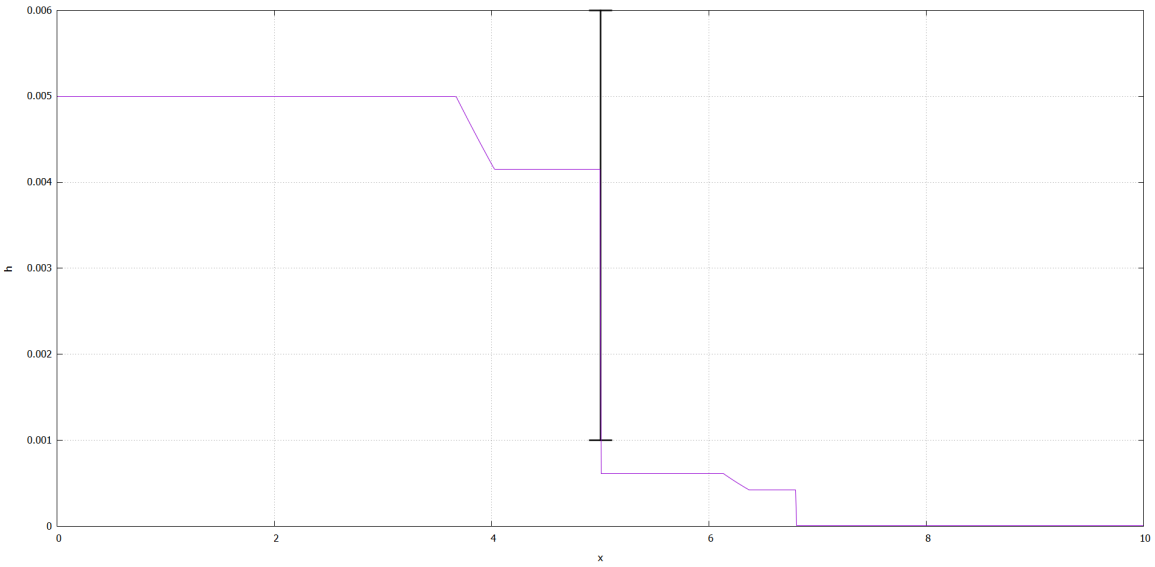

Figure 14: Free flow solution on slightly wet domain ($h_R < h_c$) at $t = T = 6$ s.

2.2.3 Free flow solution on wet domain ($h_c < h_R \leq b$)

We here take a look at the second case of free flow on wet floor where $h_c < h_R \leq b$. If $h_R > b$ we then find a submerged flow, this solution is covered in Cozzolino et al. (2015). The solution upstream of the dam is the same as for the dry domain, we still have $\mathbf{U}_L$ and $\mathbf{U}_1$ linked by a rarefaction wave. We find $\mathbf{U}_1$ at the intersection between $R(\mathbf{U}_L, \mathbf{U})$ and $FF(\mathbf{U})$. Downstream, we obtain a new intermediate state $\mathbf{U}_2$ between $\mathbf{U}_c$ and $\mathbf{U}_R$, with $h_c < h_R < h_2$. The solution is of the form:

$$\mathbf{U}_L \xrightarrow{R} \mathbf{U}_1 \xrightarrow{CD} \mathbf{U}_c \xrightarrow{S} \mathbf{U}_2 \xrightarrow{S} \mathbf{U}_R.$$

We find $\mathbf{U}_c$ on $CD(h_1u_1, \mathbf{U})$ individuated by $h_c = C_cb$. Finally, $\mathbf{U}_2$ is found at the intersection between the curves $S(\mathbf{U}_c, \mathbf{U})$ and $S(\mathbf{U}, \mathbf{U}_R)$, be wary to use the right sign, $h_c < h_R < h_2$. We obtain the following solution:

$$h(x,t) = \begin{cases} h_L \\ \frac{1}{9g}\left(2\sqrt{gh_L} - \frac{x-x_0}{t}\right)^2 \\ h_1 \\ h_c \\ h_2 \\ h_R \end{cases} \qquad u(x,t) = \begin{cases} 0 & \text{if } x \leq x_1(t) \\ \frac{2}{3}\left(\sqrt{gh_L} + \frac{x-x_0}{t}\right) & \text{if } x_1(t) \leq x \leq x_2(t) \\ u_1 & \text{if } x_2(t) \leq x \leq x_0 \\ u_c & \text{if } x_0 \leq x \leq x_3(t) \\ u_2 & \text{if } x_3(t) \leq x \leq x_4(t) \\ 0 & \text{if } x_4(t) < x, \end{cases}$$

where:

- $x_0 = 5$ m
- $x_1(t) = x_0 - t\sqrt{gh_L}$
- $x_2(t) = x_0 - t(3\sqrt{gh_1} - 2\sqrt{gh_L})$
- $x_3(t) = x_0 + t\left(u_c - h_2\sqrt{\frac{g}{2}\left(\frac{1}{h_c} + \frac{1}{h_2}\right)}\right)$

- $x_4(t) = x_0 + t\left(u_2 + h_R\sqrt{\frac{g}{2}\left(\frac{1}{h_2} + \frac{1}{h_R}\right)}\right)$.

In SWASHES, we set $h_L = 0.005$ m, $b = 0.2h_L$, $h_R = 0.2h_L$ and $C_c = 0.611$. This solution is represented at $t = T = 6$ s, in figure 15.

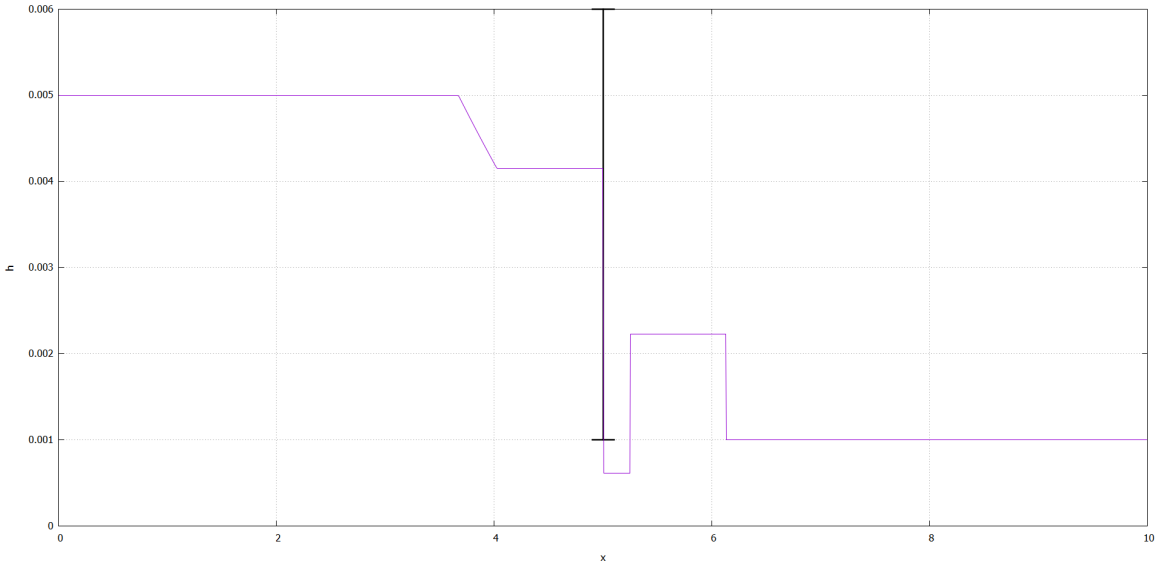

Figure 15: Free flow solution on wet domain ($h_c < h_R \leq b$) at $t = T = 6$ s.

2.3 Dam break problem with a step

In this section we consider the Riemann problem applied to a dam break with a discontinuous jump in the topography at the dam, we call it the step. We solved the classical Riemann problem in section 2.1 and defined several useful equations and notations that we reuse in this section. This section is mostly based on Han and Warnecke (2014).

We recall the setting: We consider a domain in one dimension, divided in its center by a dam represented by a discontinuity between the left state and the right state, in this case we also add a discontinuity in the topography at the dam. We note x_0 the position of the dam and the step, we note $\mathbf{U}_L = (h_L\ u_L)^T$ and $\mathbf{U}_R = (h_R\ u_R)^T$ the left side and right side states. For this solution, we also note z_L and z_R the height of the topography on the left and right side respectively. We can write the problem as follows:

$$\mathbf{U}(x,0) = \begin{cases} \mathbf{U}_L,\ x < x_0 \\ \mathbf{U}_R,\ x > x_0 \end{cases} \qquad z(x) = \begin{cases} z_L,\ x < x_0 \\ z_R,\ x > x_0. \end{cases}$$

In the rest of the section we consider $z_L = 0$ and $z_L \leq z_R$ without loss of generality, to find a solution with $z_L > z_R$, one just needs to apply a symmetry at center with the analytical solution.

We consider here the frictionless Shallow-Water equations. A word of caution must be expressed here. It is apparent that the water close to the step is neither frictionless, nor can be assumed to fulfill the approximations required for the Shallow-Water equations. In reality, a recirculation flow appears in the vicinity of the step as shown on figure 16, where for example the speed component along the z-axis is clearly not zero. One can however consider the flow far enough upstream and downstream of the step where it is accommodated to Shallow-Water assumptions. Thus, we consider here an idealized step flow as shown on figure 17, for which energy losses are neglected (this condition can be relaxed, see Alcrudo and Benkhaldoun (2001)). With those hypotheses, it is possible to find the analytical solution of the problem.

In the idealized case, a discontinuity in water heights and speed appears at the step, similar to a stationary shock wave. We will note this wave *SST* (Steady Step Transition). Since we consider the transition to be steady, we obtain the following system by adapting (1):

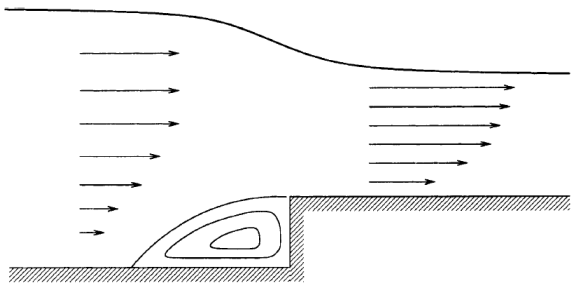

Figure 16: Actual steady flow over a step. Source: Alcrudo and Benkhaldoun (2001).

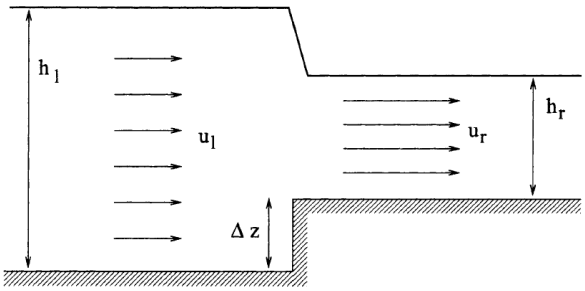

Figure 17: Idealized steady flow over a step. Source: Alcrudo and Benkhaldoun (2001).

$$\begin{cases} \partial_x h = 0 \\ u\partial_x u + g\partial_x h = -g\partial_x z. \end{cases}$$

It is possible to obtain the relation linking the states $\mathbf{U}_1$ and $\mathbf{U}_2$ on each side of the standing wave, we note this system $SST(\mathbf{U}_1, \mathbf{U}_2)$:

$$SST(\mathbf{U}_1, \mathbf{U}_2) : \begin{cases} u_1 h_1 = u_2 h_2 \\ \dfrac{u_1^2}{2} + g(h_1 + z_1) = \dfrac{u_2^2}{2} + g(h_2 + z_2). \end{cases}$$

Physically the first equation corresponds to the conservation of the discharge while the second one corresponds to the conservation of the energy. For a given state $\mathbf{U}_1$, the system might get two compatible states $\mathbf{U}_2$. One can show that a transition from a subcritical flow ($Fr = \dfrac{u}{\sqrt{gh}} < 1$) to a supercritical flow ($Fr > 1$) or vice versa can only occur at points of maximum of the bottom function (Alcrudo and Benkhaldoun 2001). Since our topography does not contain a maximum, such transitions between states are forbidden. We use this to find the only physically acceptable state linked to $\mathbf{U}_1$, since $\mathbf{U}_2$ must respect $\text{sign}(u_1^2 - gh_1) = \text{sign}(u_2^2 - gh_2)$.

Once we defined those equations, we only need to find the number of steady states and the kind of wave linking each one to entirely know the solution. We here chose to implement the case where intial speed are null and $h_L > h_R + z_R$. In such cases, we find a solution similar to the one for the dam break problem without a step 2.1.2, with an added discontinuity caused by the step:

$$\mathbf{U}_L \xrightarrow{R} \mathbf{U}_1 \xrightarrow{SST} \mathbf{U}_2 \xrightarrow{S} \mathbf{U}_R.$$

Here we reuse the equations defined in section 2.1.1. Analogously to the opening of a sluice gate (see 2.2.1), $\mathbf{U}_1$ is found at the intersection between $R(\mathbf{U}_L, \mathbf{U})$ and $SST(\mathbf{U}, \mathbf{U}_2)$ where $\mathbf{U}$ is the state we search. The added difficulty here being that $\mathbf{U}_2$ is unknown as well. However we know that $\mathbf{U}_2$ lies on the curve $S(\mathbf{U}, \mathbf{U}_R)$. Knowing that $h_L > h_1 > h_2 > h_R$ and $u_L = u_R = 0$, we can obtain the following system:

$$\begin{cases} u_1 = 2\sqrt{gh_L} - 2\sqrt{gh_1} \\ u_2 = \sqrt{\frac{g}{2}(h_2 - h_R)^2 \left(\dfrac{1}{h_2} + \dfrac{1}{h_R}\right)} \\ h_1 u_1 = h_2 u_2 \\ \dfrac{u_1^2}{2} + g(h_1 + z_1) = \dfrac{u_2^2}{2} + g(h_2 + z_2). \end{cases} \tag{8}$$

The first two lines correspond to $R(\mathbf{U}_L, \mathbf{U}_1)$ and $S(\mathbf{U}_2, \mathbf{U}_R)$, while the other two correspond to $SST(\mathbf{U}_1, \mathbf{U}_2)$. By injecting the first two lines in the last two lines, with $z_1 = 0$ and $z_2 = z_L$, we define

the following function:

$$\Gamma(h_1,h_2)=\begin{cases}h_1(2\sqrt{gh_L}-2\sqrt{gh_1})-h_2\sqrt{\frac{g}{2}(h_2-h_R)^2\left(\frac{1}{h_2}+\frac{1}{h_R}\right)}\\ 2(\sqrt{gh_L}-\sqrt{gh_1})^2-\frac{g}{4}(h_2-h_R)^2\left(\frac{1}{h_2}+\frac{1}{h_R}\right)+g(h_1-h_2-z_R).\end{cases}$$

We then search for the point $\Gamma(h_1,h_2)=(0,0)^T$ using any iterative method, to obtain h_1 and h_2. We can then obtain u_1 et u_2 with (8). To solve the system, one can for example use Sagemath, or any other numerical methods. We give an example of Sagemath code in figure 18.

```
reset()
hr = 1
hl = 4
g = 9.81
z = 1
var('h1,h2')
solve([h1*(2*sqrt(g*hl)-2*sqrt(g*h1))-h2*sqrt(g/2*(h2-hr)^2*(1/h2+1/hr))==0,
    (2*sqrt(g*hl)-2*sqrt(g*h1))^2/2+g*h1-g/4*(h2-hr)^2*(1/h2+1/hr)-g*(h2+z)==0],
    h1,h2)
```

Figure 18: Example of Sagemath code to search for the values h_1 and h_2 such that $\Gamma(h_1,h_2)=(0,0)^T$.

Once we found $\mathbf{U}_1$ and $\mathbf{U}_2$, the solution is entirely known:

$$h(x,t)=\begin{cases}h_L\\ \frac{1}{9g}\left(2\sqrt{gh_L}-\frac{x-x_0}{t}\right)^2\\ h_1\\ h_2\\ h_R\end{cases}\qquad u(x,t)=\begin{cases}0 & \text{si } x\le x_1(t)\\ \frac{2}{3}\left(\sqrt{gh_L}+\frac{x-x_0}{t}\right) & \text{si } x_1(t)\le x\le x_2(t)\\ u_1 & \text{si } x_2(t)\le x\le x_0\\ u_2 & \text{si } x_0\le x\le x_3(t)\\ 0 & \text{si } x_3(t)<x,\end{cases}$$

where:

- $x_1(t)=x_0-t\sqrt{gh_L}$
- $x_2(t)=x_0-t(3\sqrt{gh_1}-2\sqrt{gh_L})$
- $x_3(t)=x_0+t\left(u_2+h_R\sqrt{\frac{g}{2}\left(\frac{1}{h_2}+\frac{1}{h_R}\right)}\right)$.

The solution with the parameters chosen in SWASHES is drawn on figure 19. We set $h_L=4$ m, $h_R=1$ m, $z_R=1$ m and $T=1$ s. A word of caution for this solution in SWASHES, one should not change the parameters fixed in SWASHES. In order to keep to code as light as possible, we chose to solve (8) outside of SWASHES, so unlike every other solution in SWASHES, the given solution for this problem is only correct for $h_L=4$ m, $h_R=1$ m, $z_R=1$ m.

3 Some numerical results: comparison with FullSWOF numerical solutions

SWASHES was originally created to test FullSWOF (Delestre et al. 2017), a software for the resolution of Shallow-Water equations, and to verify it against analytic solutions. To illustrate the use of some of the new solutions we implemented in this paper, we use them to test FullSWOF.

In this section, we run FullSWOF on the dam in 2D cases (see section 1.1). We are not able to test the other new solutions because FullSWOF does not support the spherical coordinate system (see section 1.2), and the sluice gate problem requires a modified solver to account for the discontinuity at the gate opening (see section 2.2).

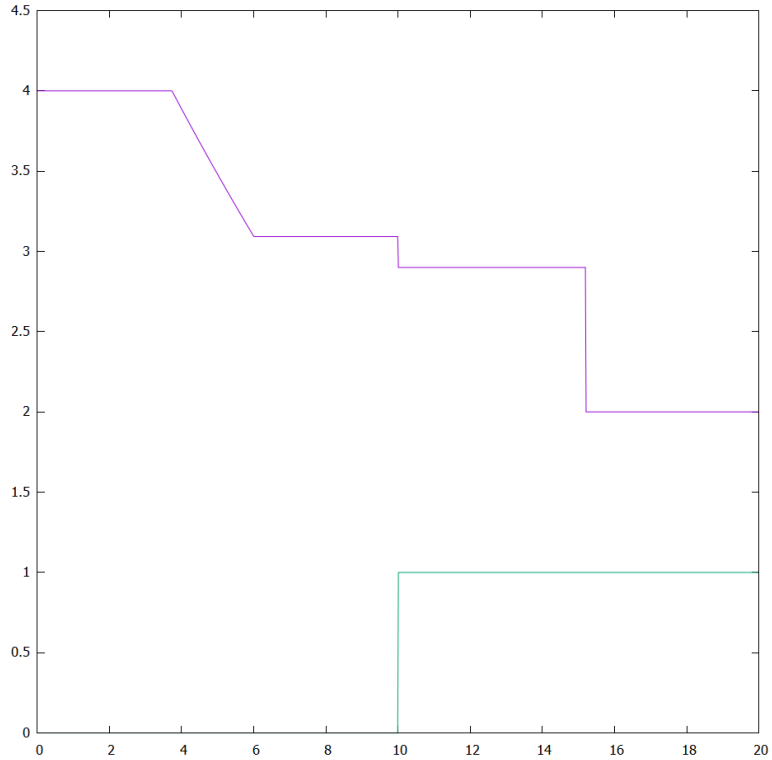

Figure 19: Solution to the dam break problem with a step, $h_L = 4$ m, $h_R = 1$ m and $z_R = 1$ m at $t = T = 1$ s.

3.1 Analysis of the FullSWOF_2D result for the parabolic dam

We tried the solver FullSWOF_2D (Delestre et al. 2017) on the parabolic dam (section 1.1.1) with initial conditions:

$$h + z = 1 \text{ m} \ , \ u = v = 0 \text{ m s}^{-1},$$

with walls on all sides apart for the downstream limit ($x = 25$ m) where we want the water to evacuate. We set the mesh as follows: $N_x = 40$ points and $N_y = 20$ points.

After 100 000 s we get the graph shown on figure 20.

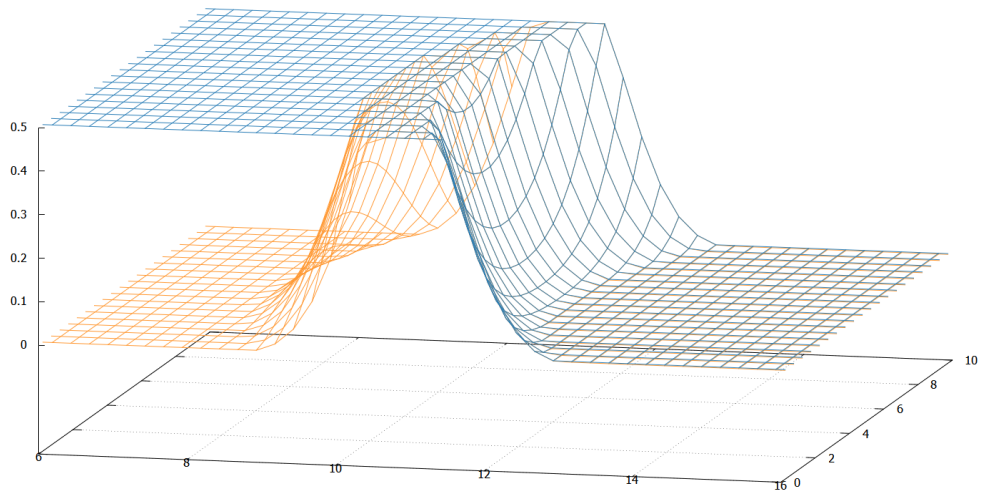

Figure 20: State of the simulation after 100 000 s.

The result from FullSWOF is close to the expected steady state. Upstream of the dam the numerical result is exact: the velocity is null, and the water is perfectly flat with $h+z = 0.5$ m. Downstream

of the dam, there is still around 2 mm of water remaining and struggling to be evacuated: between $t = 77\ 777$ s and $t = 100\ 000$ s, the water at $x = 25$ m lowered by only around 0.5 mm. This can be explained by the small values of the remaining velocity of order 10^{-4} m s^{-1} at the final time in the dry zone. It could be relevant to try running the solver for longer.

This problem is frequently encountered by solvers, showing the pertinence of this test to compare them together.

Another side of the test is the symmetry. Since the topography and the initial conditions are all symmetrical around the axis $y = l/2$, the numerical result should be symmetrical too. Here the water height in the dry zone isn't perfectly flat or symmetrical with relatively negligible differences of order 5×10^{-5} m, see figure 21. Differences of the same magnitude can be observed for u and v of order 5×10^{-5} m s^{-1} which isn't relatively negligible anymore since it corresponds to the order of u and v. Those differences cause the velocity vectors to act strangely. We even observe water going upstream (see figure 22).

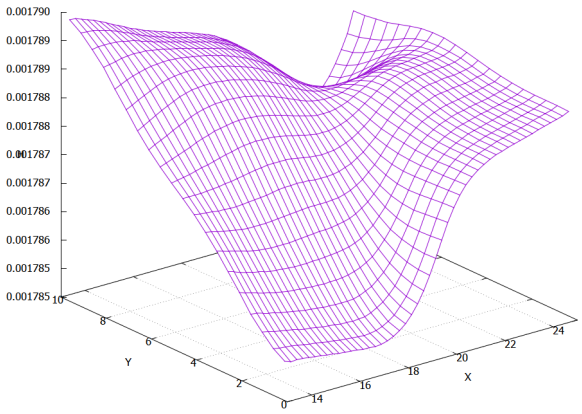

Figure 21: Water surface given by FullSWOF_2D in the dry zone ($x > 13$ m).

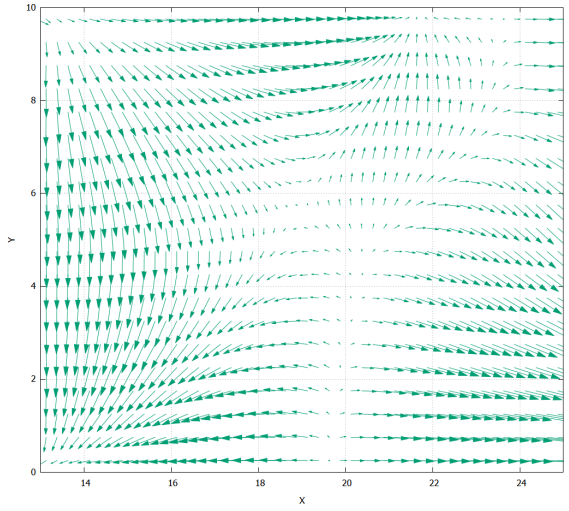

Figure 22: Speed field (multiplied by a factor 10^4) given by FullSWOF_2D in the dry zone.

3.2 Applying FullSWOF_2D to the cross-shaped dam

We tried the solver FullSWOF_2D (Delestre et al. 2017) on the cross-shaped dam (section 1.1.2) with initial conditions:

$$h + z = 1.5 \text{ m} \ , \ u = v = 0 \text{ m s}^{-1}.$$

For the boundary conditions, we do not set any walls and let the water escape from all sides ($h = 0$ is imposed). We set the mesh as follows: $N_x = N_y = 50$ points. The state of the numerical solution at the final time $t = 10\ 000$ s is shown on figure 23.

The result from FullSWOF is close to the expected steady state. In the well pit, the solution is exact with $h + z = 1$ m and $u = v = 0$ m s^{-1}. We have h close to 0 everywhere else. Aside for the flat ridge around the well, h either equals 0 or is of order, 2×10^{-12} m which is clearly negligible. This result can be explained by the implementation of FullSWOF. Since it is hard to obtain a true 0 with a numerical solver, a certain $\epsilon = 10^{-12}$ m (which can be considered as the machine error) has been introduced. In FullSWOF, if $h < \epsilon$ we consider $h = 0$ m. As for the velocities, they are of order 2 m s^{-1} in this zone and pointed outwards, which explains why the water did not struggle to evacuate as much as it did for the parabolic dam (see section 3.1), probably thanks to the flat dry surface being much shorter.

Apart for the inside of the well where $h + z = 1$ m, the only zone with water height above 10^{-11} m is the flat ridge around the well, where h is of order 10^{-8} m, which can be explained by the low velocity in those points of order 10^{-5} m s^{-1} (see figure 25).

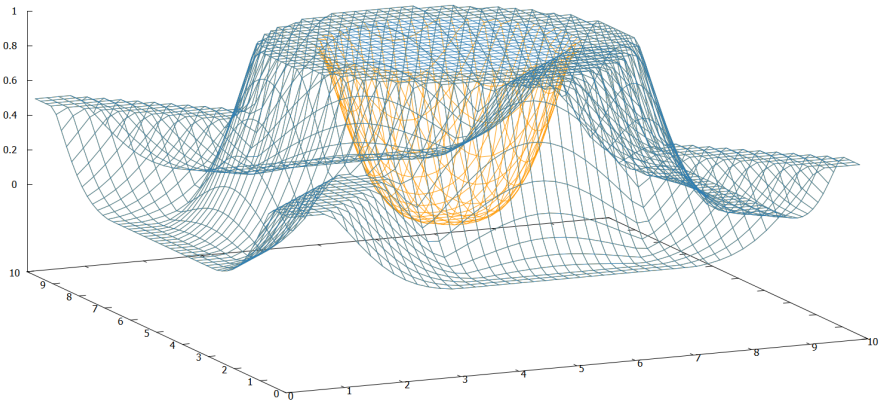

Figure 23: State of the simulation after 10 000 s.

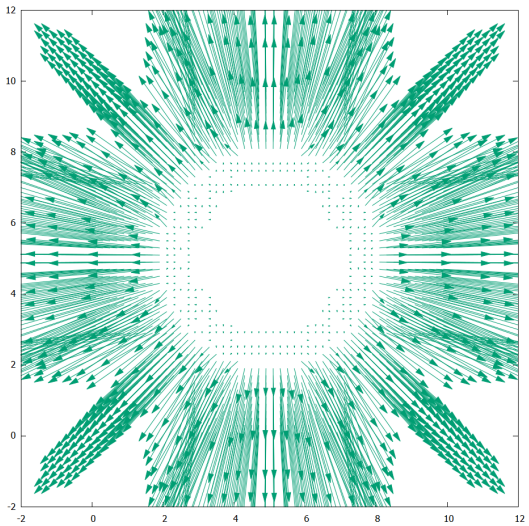

Figure 24: Speed field at final time given by FullSWOF_2D.

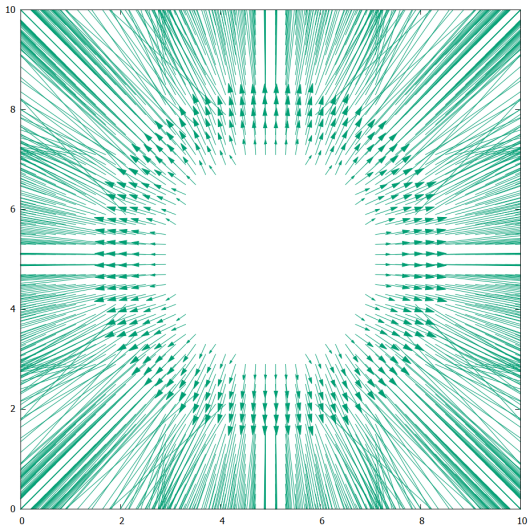

Figure 25: Speed field at final time (multiplied by 10^4) centered on the central ring.

The main interest of this test was to check the symmetry of the numerical solution. Since the topography and the initial conditions are all symmetric along the horizontal axis, the vertical axis, $x = y$ and $x = -y$, the numerical solution should be symmetric as well. It is almost the case for all axes with an error of order ϵ which is negligible, see for example for the velocity on figure 24.

3.3 Applying FullSWOF_1D to the dam break over a step

We tried the solver FullSWOF_1D on the dam break over a step problem (section 2.3). We expect the discontinuity of the topography to be a problem. We keep the initial value, $h_L = 4$ m, $h_R = 1$ m and we keep $z_R = 1$ m. We set the mesh as follows: $N_x = 200$ points. The comparison between the analytic solution and the result of FullSWOF_1D, at $t = 1$ s, are shown on figure 26.

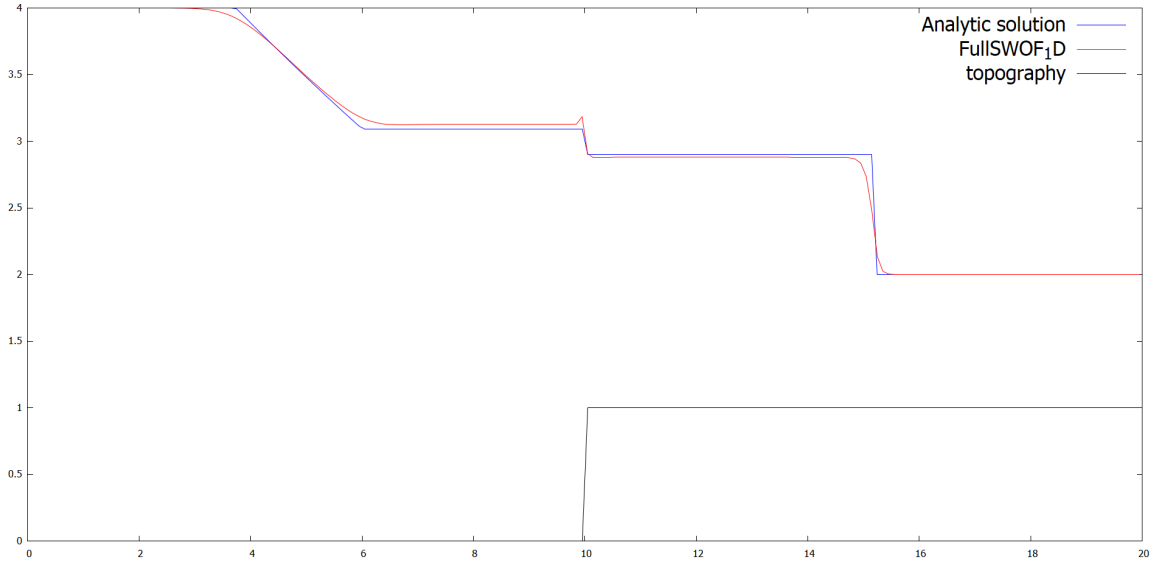

Figure 26: Comparison between FullSWOF_1D and the analytic solution at $t = 1$ s.

4 Conclusion

We expanded SWASHES with 8 new solutions to the software at version 1.04.00. They complete the already implemented stationary and transitory solutions. They allow testing adapted solvers, such as a solver functioning in the spherical coordinate system, as well a solver adapted to the specific Riemann problem. With the base code for spherical coordinate system now implemented, it will be rather easy to implement new spherical analytical solutions in future version of the software.

5 References

Alcrudo, F. and Benkhaldoun, F. (2001). "Exact solutions to the Riemann problem of the shallow water equations with a bottom step". In: *Computer & Fluids* 30.6, pp. 643–671. DOI: 10.1016/S0045-7930(01)00013-5.

Cozzolino, L., Cimorelli, L., Covelli, C., Della Morte, R., and Pianese, D. (2015). "The analytic solution of the Shallow-Water Equations with partially open sluice-gates: The dam-break problem". In: *Advances in Water Resources* 80, pp. 90–102. DOI: 10.1016/j.advwatres.2015.03.010.

Delestre, O., Lucas, C., Ksinant, P.-A., Darboux, F., Laguerre, C., Vo, T.-N.-T., James, F., and Cordier, S. (2013). "SWASHES: a compilation of Shallow Water Analytic Solutions for Hydraulic and Environmental Studies". In: *International Journal for Numerical Methods in Fluids* 72.3, pp. 269–300. DOI: 10.1002/fld.3741.

Delestre, O., Darboux, F., James, F., Lucas, C., Laguerre, C., and Cordier, S. (2017). "FullSWOF: Full Shallow-Water equations for Overland Flow". In: *Journal of Open Source Software* 2.20, p. 448. DOI: 10.21105/joss.00448.

Han, E. and Warnecke, G. (2014). "Exact Riemann solutions to shallow water equations". In: *Quarterly of applied mathematics* 72.3, pp. 407–453. DOI: 10.1090/S0033-569X-2014-01353-3.

LeVeque, R. J. (2002). *Finite Volume Methods for Hyperbolic Problems*. Cambridge University Press. DOI: 10.1017/CBO9780511791253.

Mecholic (2018). *What is vena contracta? How vena contracta formed in fluid flow?* URL: https://www.mecholic.com/2018/11/what-is-vena-contracta.html.

Williamson, D. L., Drake, J. B., Hack, J. J., Jakob, R., and Swarztrauber, P. N. (1992). "A standard test set for numerical approximations to the shallow water equations in spherical geometry". In: *Journal of Computational Physics* 102, pp. 211–224. DOI: 10.1016/S0021-9991(05)80016-6.